BLOCK SHEAR MODEL FOR AXIALLY-LOADED GROUPS OF SCREWS

Ursula Mahlknecht[1)*)], Reinhard Brandner[1)], Andreas Ringhofer[1)]

[1)] Institute of Timber Engineering and Wood Technology, Graz University of Technology, Graz, Austria, [*)] u.mahlknecht@tugraz.at

This paper was originally published for INTER 2022.

Keywords: axially-loaded groups of screws, hanger loaded perpendicular-to-grain, block shear failure mechanism, load sharing

1 INTRODUCTION

Primary axially-loaded screw groups inserted perpendicular- or under an angle-to-the-grain of structural timber elements, see Figure 1.1 (left), cause locally shear, rolling shear and tensile perpendicular-to-the-grain stresses. Under certain conditions, these stresses lead to brittle joint failure mechanisms in timber, such as tension perpendicular-to-the-grain (splitting), row or block shear. The row shear failure mechanism is characterised by tearing out of narrow timber slices in-between the rows of screws parallel-to-the-grain; see Figure 1.3 (right). Carradine (2009), Plieschounig (2010), Mayer and Blaß (2018), Blaß et al. (2019), Blaß and Flaig (2019) and Mahlknecht et al. (2021) observed row shear in their tests in Norway spruce at $a_1 < 5\ d$ as well as in some hardwoods at $a_1 \leq 5\ d$. The block shear failure mechanism constitutes a combined rolling shear / shear and tensile perpendicular-to-the-grain failure of the timber volume comprising the entire screw group; see Figure 1.1 (middle and right). Compared with failure mechanisms analogue to that of single screws, e.g. withdrawal or steel tension failure, these brittle timber failure mechanisms are less predictable and have the potential to significantly reduce the resistance and reliability of such joints. This is because of their high complexity due to the large number of parameters describing the material, geometry and stress distribution, as outlined in the following, and the still missing engineering models, which allow verification of these potential failure mechanisms for all the possible joint configurations.

The focus of this contribution is on the block shear failure mechanism for common rectangular designs of screw groups. The block shear volume is principally limited in depth by the penetration length l_p, as sum of the effective threaded length l_{ef} (threaded length without tip length l_{tip}) and embedment length l_{emb}, and in plane by the circumference of the screw group; typically characterizing cracks are shown in Figure 1.1 (middle and right). This failure mechanism has to be differentiated from the block shear failure mechanisms associated with groups of laterally-loaded dowel-type fasteners, which are frequently addressed in literature. The block shear failure mechanism of axially-loaded screw groups could be observed for $\alpha = 90°$ and even for screw groups inserted in timber members at an angle between the screw axis and the grain of 45° and loaded axially in tension. This although the minimum geometric conditions were met acc. to EN 1995-1-1 (2014; EC 5) and SIA 265 (2021), with $(a_1 \mid a_2 \mid a_{2,CG}) / d = (7 \mid 5 \mid 4)$, as well as acc. to various ETAs of well-known screw producers, with $(a_1 \mid a_2 \mid a_{2,c)} / d \geq (5 \mid 2.5 \mid 3)$ and $a_1\ a_2 \geq (21)\ 25\ d^2$; see e.g. Mahlknecht and Brandner (2013), Mahlknecht et al. (2014), Ringhofer and Schickhofer (2015), Mahlknecht et al. (2016), Mahlknecht and Brandner (2019) and Blaß and Flaig (2019). The referenced test series comprise Norway spruce (Picea abies), various timber products (solid timber; glulam (GLT); cross laminated timber (CLT)), self-tapping screws, various geometrical parameter settings and test configurations (near; in-between; distant supports); see Figure 1.2. Recently, Mahlknecht et al. (2021) reported a similar behaviour also for screw groups in solid timber, glulam and laminated veneer lumber (LVL) made of hardwood.

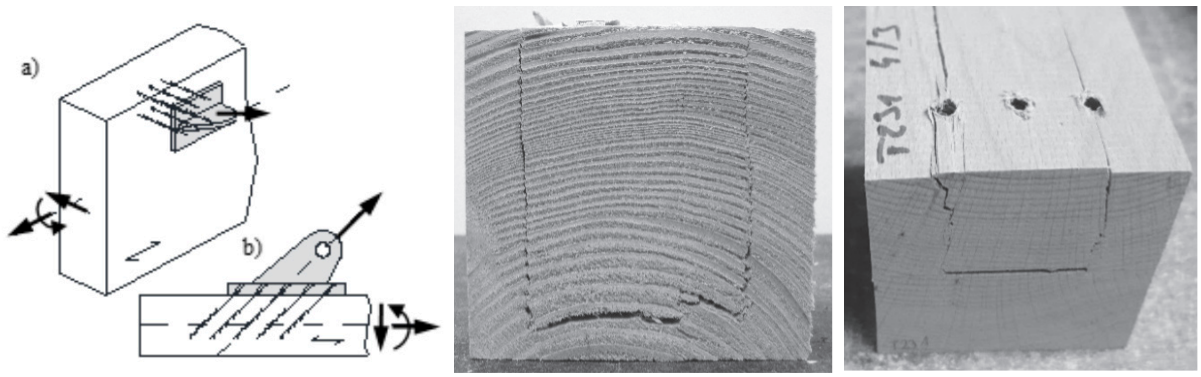

Figure 1.1 (left) examples for unilateral joints of primary axially-loaded screw groups with a risk for block shear failure mechanism: a) wind bracing joint on side-face and b) hangered beam; (middle); typical block shear failure pattern on a cross section cut in the middle of a screw joint, exemplarily for a group of 5 x 5 screws in Norway spruce and (right) for a group of 3 x 5 screws in birch.

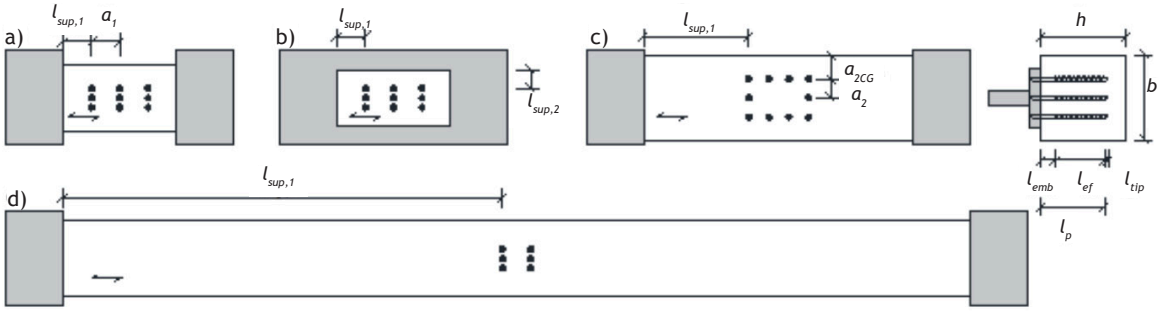

Figure 1.2 Schematic view on the dimensions of tested screw groups at a = 90° with a) near end and b) near circumferential, with $l_{sup,1} \approx a_1$ and $l_{sup,2} \approx a_2$, respectively, c) in-between, with $l_{sup,1} \approx h$, and d) distant supports, with $l_{sup,1} \approx 3\,h$.

Block shear failures were commonly observed in joints (i) with outer steel plates taking off when loaded (see Figure 1.1, left) together with (ii) tight group designs, i.e. screw groups featuring small spacings parallel- (a_1) and especially perpendicular-to-the-grain ($a_2 < 5\,d$). Thereby, failure patterns with clear block shear cracks (see Figure 1.3 a)) and in addition that alike of Figure 1.3 b) and c) were observed and due to their overall characteristic brittle load-deformation curves assigned to block shear.

EC 5 (2014) and SIA 265 (2021) demand the verification of block shear also for axially-loaded screw groups; but related design rules are not provided. In the same context, the current draft of prEC 5 (2021) does not address this failure mechanism at all explicitly. Anyway, EC 5 (2014), based on Leijten and Jorissen (2001), provides design provisions against splitting for joints of laterally-loaded dowel-type fasteners loading hangers perpendicular-to-the-grain. The national annexes of Austria (ÖNORM B 1995-1-1, 2019) and Germany (DIN EN 1995-1-1/NA, 2013) provide for laterally loaded fasteners and also for joints with axially-loaded glued in rods a design provisions based on Ehlbeck et al. (1989) and note, that the risk of splitting can be neglected as long as the distance from loaded timber end to the farthest fastener h_e is ≥ 0.7 h, with h as the depth of the beam. The same provisions apply for axially-loaded glued-in rods or screws in SIA 265 (2021) and prEC 5 (2021), correspondingly equating $h_e = l_p$; see also Dietsch and Brandner (2015). However, there is experimental evidence that block shear failure may occur even in joints fulfilling $l_p \geq 0.7\,h$; see Mahlknecht and Brandner (2013) and (2019).

In case of block shear failures so far there have been no fractures/cracks visible in the transversal shear planes. Considering this, Blaß et al. (2019) proposed to reduce the verification of block shear to (i) tension-perpendicular-to-the-grain (splitting) of the timber member at plane of the screw tips following the approach in EC 5 (2014) for hangers, and (ii) rolling shear at the planes of both outer screw rows parallel-to-the-grain; see Figure 1.3 (d); e)). Their approach appears to be especially suitable for screw groups with >> l_p and edge distances close to $a_{2,CG}$. The validation of their suggested parameters, as the effective widths and lengths of the potential failure planes, remains open for a broader range of screw groups, especially for joints in deep beams and/or joints with embedded screw threads ($l_{emb} > 0$; see Figure 1.2).

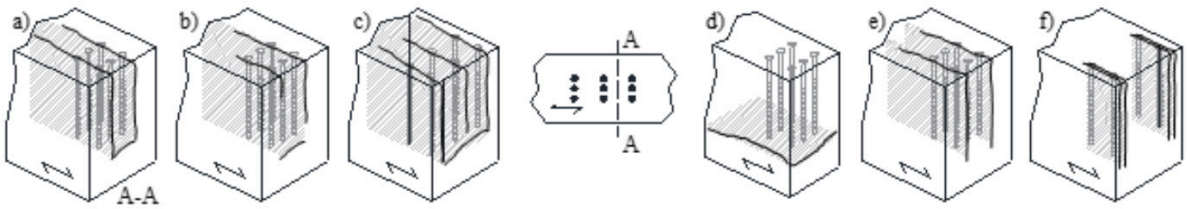

Figure 1.3 Schematic illustration of potential brittle timber fracture patterns in case of in tension axially-loaded screw groups: block shear failure mechanisms as defined by Mahlknecht and Brandner (2019) featuring a) clear, b) partial and c) clear and additional crack pattern; d) tension perpendicular-to-the-grain, and e) rolling shear failure mechanism as described in Blaß et al. (2019); (f) row shear failure mechanism.

2 BLOCK SHEAR MODEL OF MAHLKNECHT ET AL. (2014) AND EXTENSIONS

2.1 Basic Principles

The block shear model of Mahlknecht et al. (2014) and subsequent extensions represent in a way an analogy to the block shear model for parallel-to-the-grain loaded joints of laterally-loaded rivets from Zarnani and Quenneville (2012). Mahlknecht et al. (2014) basically describe the resistance of a timber member at the joint against block shear by means of a parallel system of in total five planes: two planes each acting against transversal shear ($A_{s,s}$) and rolling shear ($A_{s,r}$) at the circumference of the screw group and one plane at the tips resisting tensile-stresses perpendicular-to-the-grain ($A_{t,90}$); see Eq. (1) and Figure 2.1. These equations contain a_1 and a_2, s and r are the numbers of screws in a row perpendicular- and parallel-to-the-grain, respectively, and h_b is the depth of the block shear volume, which may differ from the penetration length l_p (see Section 2.2). To account for the proportional contribution of these planes in load sharing and redistribution, corresponding stiffnesses, i.e. parallel acting springs, are defined by assuming a uniform deformation Δ as well as a linear-elastic and quasi-brittle material behaviour; see Eqs. (2) to (4). In doing so, the elastic material properties (Young's modulus perpendicular-to-the-grain $E_{t,90}$ and shear moduli G_0 and G_r) as well as stress distribution parameters are defined: $C_{t,90}$, to describe the ratio of a non-uniform to a uniform tensile stress distribution over h_b, C_t, C_s and C_r, to account for the non-uniform stress distribution along the corresponding planes, and X_s and X_r as lengths of the lateral volume parallel and perpendicular-to-the-grain, respectively, which are activated by the shear deformations; see Figure 2.1.

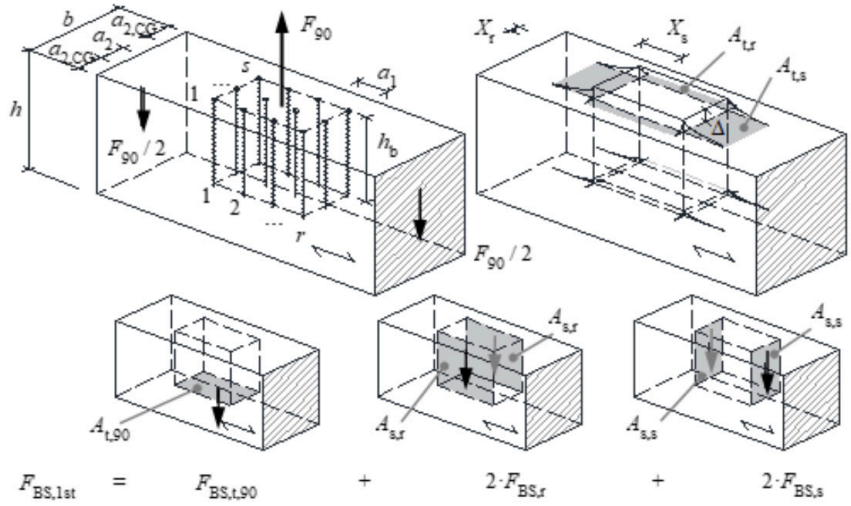

Figure 2.1 Contributing planes and geometric parameters of the block shear model for a group of axially-loaded screws together with some schematic assumptions.

$$A_{t,90} = (r - 1)\, a_1\, (s - 1)\, a_2;\ A_{s,s} = (s - 1)\, a_2\, h_b;\ A_{s,r} = (r - 1)\, a_1\, h_b \quad (1)$$

$$K_{t,90} = E_{t,90}\, A_{t,90} / (C_{t,90}\, h_b) \quad (2)$$

$$K_s = G_0\, A_{s,s} / X_s + E_{t,90}\, A_{t,s} / (10\, h_b),\ \text{with}\ A_{t,s} = (s - 1)\, a_2\, X_s \quad (3)$$

$$K_r = G_r\, A_{s,r} / X_r + E_{t,90}\, A_{t,r} / (10\, h_b),\ \text{with}\ A_{t,r} = (r - 1)\, a_1\, X_r \quad (4)$$

Due to the assumed parallel system action together with linear-elastic and (quasi) brittle material behaviour, the maximum load at 1st failure, $F_{BS,1st} = K_{1st}\ e_{f,(1)}$, corresponds to the resistance of the system at the deformation at 1st fracture $e_{f,(1)} = \min(e_{f,(i)})$, with $e_{f,(i)} = C_i\ f_i\ A_i\ /\ K_i$ and $K_{1st} = K_{t,90} + 2\ K_s + 2\ K_r$. This coincides with the corresponding strength f_i ($f_{t,90}$ tension perpendicular-to-the-grain, f_v shear or f_r rolling shear strength) at the corresponding (theoretically potential) failure plane(s) A_i ($A_{t,90}$, 2 $A_{s,r}$ or 2 $A_{s,s}$); see Figure 2.2. Subsequent maximum loads of remaining planes, which are still active in load sharing, can be calculated analogously; see Mahlknecht and Brandner (2019) and Figure 2.2. The overall maximum load the block can resist, is consequently given as the maximum of these intermediate maxima. The first failure criterion was directly derived from test observations. Also there, first (partial) failures associated with load drop and stiffness loss, followed by further load increase, were observed. This phenomenon, however, was not observed in all tests; some of them failed without these apparent first failures. Because of the uncertainty related to the residual long-term capacity of already partially failed timber volumes at such joints, for the design models presented and discussed further only $F_{BS,1st}$ is considered. More details are provided in Mahlknecht and Brandner (2019) and Mahlknecht (pr 2023).

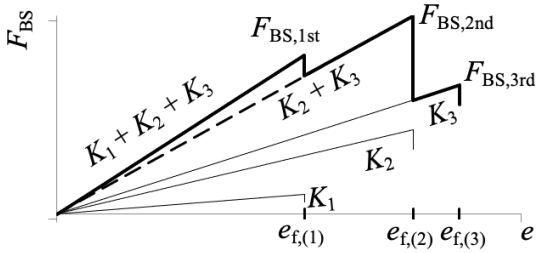

Figure 2.2 Schematic load-deformation-curves in case of block shear failure with suczessive, linear-elastic and (quasi) brittle material behaviour acc. to Mahlknecht and Brandner (2019).

2.2 Model parameters

Accomprehensive discussion on the model parameters based on Mahlknecht et al. (2014) and (2016) is given in Mahlknecht and Brandner (2019). The basic parameter settings are listed in Table 2.1 and Table 2.2. Because of well-known size effects, values for $f_{t,90}$ and f_v are related to the dimensions of $A_{t,90}$ and $A_{s,s}$. As the position of the failure plane, it's depth, in clearly defined, $f_{t,90}$ relates to solid timber without pith. The stress distribution parameters were determined on the basis of a mechanical approach analogue to compression perpendicular-to-the-grain together with FE-and test data analysis. Latter is done in particular as decision aid for the dimension of X_s and X_r by a classification between block shear and single fastener failure in dependency of the spacing. Namely, this provides the information up to which spacing (a_1 and a_2) an overlapping of inserted loads per screw is given and a conclusion alike an effective thickness or width per screw can be done.

Table 2.1 Average material properties as well as geometric and stress distribution parameter settings for the block shear model of Mahlknecht and Brandner (2019).

[N/mm²]	$f_{t,90,mean}$	$E_{t,90,mean}$	$f_{v,mean}$	$G_{0,mean}$	$f_{r,mean}$	$G_{r,mean}$
GLT	2.04 (3,150 / $A_{t,90}$)$^{0.2}$ [a]	300 [b]	40.2 $A_{s,s}^{-0.2}$ [d]	650 [b]	1.9 [f]	100 [f]
ST	2.04 (3,150 / $A_{t,90}$)$^{0.2}$ [a]	350 [c]	55.2 $A_{s,s}^{-0.22}$ [d]	690 [e]	1.9 [f]	100 [f]

[a] reference data from Blaß et al. (1998); [b] GL 24h acc. to EN 14080 (2013); [c] close to C24 acc. to EN 338 (2016); [d] acc. to Brandner et al. (2012); [e] C24 acc. to EN 338 (2016); [f] acc. to Ehrhart and Brandner (2018)

support distance	$C_{t,90}$	C_t	$C_s = C_r$	X_s	X_r
close	0.5	1.0	0.9	5 d	min(2.5 d; $l_{sup,2}$)
in-between; $l_{sup,1} \approx h$	0.5	1.0	1.0	50 mm	5 d

Mahlknecht and Brandner (2019) focused on near support conditions. Aiming on a more general application of the block shear model and supported with new data sets Mahlknecht (pr 2023) provides a complement, more specified set of parameters:

- given the predefined failure plane at the screw tips, for $f_{t,90}$ in solid timber and glulam (series h21_E) the influence of pith is neglected and $f_{t,90,mean}$ kept as in Table 2.1; for all other glulam series and by means of data from Blaß et al. (1998) $f_{t,90,mean} = 1.85\ (3{,}150 / A_{t,90})^{0.2}$ is set;
- acc. to EN 338 (2016) $E_{t,90,mean}$ for C24 is set to 370 N/mm²;
- FE-analyses in Mahlknecht (pr 2023) outline the necessity to consider $l_{emb} > 0$ in the theoretical height h_b of the block shear volume, with $h_b = l_{emb} + l_{ef}$ for near and $h_b = 0.5\ l_{emb} + l_{ef}$ for in-between and distant support conditions;
- FE-analyses showed that for in-between ($l_{sup,1} \approx h$) and distant supports ($l_{sup,1} > h$) the same values for C_s and C_r can be applied;
- X_r is corrected to 2.5 d, independent of the support distance;
- in close agreement with Mahlknecht and Brandner (2019), for distant supports and in consideration of the insertion depth $X_s = (10 - 5\ l_p / h)\ d$ is set.

Table 2.2 Coefficients of variation and correlations between material properties, Mahlknecht (pr2023).

CoV [%]	$E_{t,90}$	G_0	G_r	$f_{t,90}$	f_v	f_r
ST [a]	15	12	20	25	15	20
GLT [b]	15	12	15	25	15	20

[a] C24 acc. to EN 338 (2016); [b] GL 24h and GL 28h acc. to EN 14080 (2013)

$\rho_{Xi,Xj}$ [-]	$E_{t,90}$	G_0	G_r	$f_{t,90}$	f_v	f_r
$E_{t,90}$	1	0.6 [c]	0.6 [e)f)]	0.4 [c]	0.6 [c]	0.6 [e)f)]
G_0		1	0.2	0.4 [c]	0.6 [c]	0.2
G_r			1	0.4 [e]	0.2	0.8 [d]
$f_{t,90}$				1	0.6 [c]	0.4 [e]
f_v	symm.				1	0.2 [e]

[c] acc. to JCSS (2006); [d] analogue to $\rho(f_{t,0}; E_0)$ acc. to JCSS (2006) and similar to Ehrhart and Brandner (2018); [e] correlation measures assumed due to lack of information; [f] dependencies of $E_{t,90}$ with G_r and $E_{t,90}$ with f_r argued with the common dependency on the annual ring orientation.

In addition to the mechanical formulation of the block shear model by means of average properties and parameter settings it has been extended to a stochastic-mechanical model. This allows now to consider the corresponding uncertainties and correlations, as summarised in Table 2.2, and to formulate the block shear model also on the characteristic (5 %-quantile) level.

The material properties, expressed via the random variable vector $Y = [E_{t,90};\ G_0;\ G_r;\ f_{t,90};\ f_v;\ f_r]$, are assumed to be lognormal distributed; see JCSS (2006), except $f_{t,90}$. For the stochastic analyses of the block shear model, each series is represented by 1,000 pseudo random samples. For each sample block shear resistance $F_{BS,1st,i}$ and the corresponding theoretical failure plane are determined. Figure 2.3 left exemplarily for series s12_S illustrates the PP-plot of $\ln(F_{BS,1st})$ assuming again a normal distribution by classifying the 1,000 repetitions acc. to the three failure planes. This graph also contains the average material properties of the simulated sample and the relative shares of the three failure plane classes.

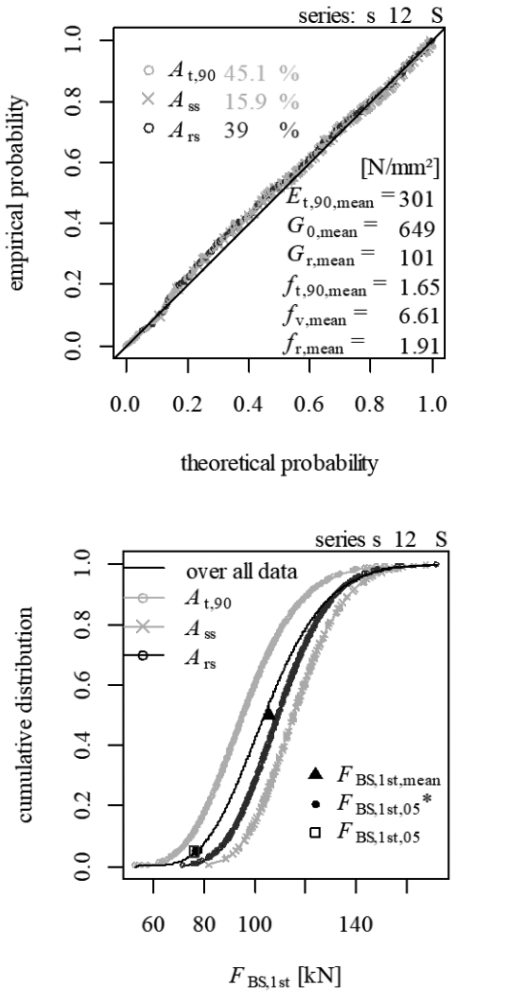

Figure 2.3 Outcomes of the stochastic-mechanical model exemplarily for series s12_S (GLT; r = 3; s = 4; d = 6 mm; a1 = a2 = 5 d; lef = 15.3 d): (left) PP-plot of ln(FBS,1st) separate for each 1st failure plane together with corresponding relative shares and the average values from the random sample; (right) cumulative distributions for the overall sample outcome and individually for each 1st failure plane class together with mean and 5 %-quantile values

From these data sets empirical mean ($F_{BS,1st,mean}$) and empirical 5 %-quantile ($F_{BS,1st,05}$) values based on rank statistics are estimated as well as the 5 %-quantiles assuming a lognormal distribution ($F_{BS,1st,05}$*). Figure 2.3 right gives the distribution function of the whole date set, the individual distributions for each class of 1st failure planes as well as the mean and both 5 %-quantile values.

The presented simulated data mirroring test series s12_S visualizes well the separation in the three classes of corresponding theoretical failure planes. In fact, in series s12_S by testing 3 / 5 joints failed in withdrawal and 2 / 5 block in block shear. Series, which ended total in block shear, show a clear responsible failure plane with a high relative frequency. The ln($F_{BS,1st}$) in Figure 2.3 left agrees widely with an assumed normal distribution, consequently, $F_{BS,1st}$ follows a lognormal distribution.

2.1 Differentiation from other failure mechanisms

The probability of occurrence for the block shear failure mechanism is, as usual, limited by all other potential failure mechanisms, e.g. withdrawal, steel failure and net cross-section failure. It is common practice in design to declare the minimum of all associated design resistances as design value for the corresponding joint. In view of the single screw failure mechanisms this corresponds to $R_{joint,d} = \min \{F_{ax,sgl,d}\ n_{ef}; F_{tens,sgl,d}\ n_{ef}\}$.

In the following, the average single screw withdrawal capacity, $F_{ax,sgl}$, is determined acc. to the model of Ringhofer et al. (2015), by taking the average density of each series into account, as well as the system coefficient k_{sys}, to consider the number of penetrated layers N. Due to the partially low number of tests per series (≥ 4 #), the corresponding 5 %-quantile values are determined by assuming a lognormal distribution and CoV[ρ] = 0.08 for solid timber and CoV[ρ] = 0.08 / $N^{0.5}$ for glulam as suggested in Ringhofer et al. (2015). The average screw tensile capacity, $F_{tens,sgl,mean}$, is available from reference tests. In calculating the 5 %-quantiles, a CoV[F_{tens}] = 0.05 and a lognormal distribution are assumed. For model validation based on tests conducted under laboratory conditions $n_{ef} = n$ is applied; see Mahlknecht and Brandner (2019). In respect to practical applications of such joints, also the regulations of EC 5 (2014) ($n_{ef} = n^{0.9}$) is applied, as well as for completeness the proposal, which apply for lap joints acc. to Krenn (2017) and regulations of various ETAs, with $n_{ef} = 0.9\ n$.

For the calculation of the resistance of screw groups against tensile stresses perpendicular-to-the-grain, Blaß et al. (2019) made the following proposal:

$$F_{t,90,Blaß} = (k_s\ h) \ /\ (h - l_p)\ (6.5 + 18\ l_p^2\ /\ h^2)\ (t_{ef}\ h)^{0.8}\ f_{t,90} \tag{5}$$

$$\text{with } k_s = \max \{1.0;\ 0.7 + 1.4\ (r - 1)\ a_1\ /\ h\} \text{ and } t_{ef} = \min \{b;\ (s - 1)\ a_2 + 6\ d;\ 6\ s\ d\} \tag{6}$$

For comparison with screw groups featuring $l_{emb} > 0$, in Eq. (5) l_{ef} is substituted by l_p.

Acc. to SIA 265 (2021) the characteristic value (design value times 1.7) for the same property can be calculated acc. to Eq. (7), by considering the effective width b_{ef} and the factor k_{ar}, with the joint length $a_r = (r - 1)\ a_1$, acc. to Eq. (8), and the factor k_{hm} interpreted of the authors acc. to Eq. (9) with the effective threaded length.

$$F_{t,90,SIA,k} = 1.7\ F_{t,90,SIA,d} = 1.7\ (8.4\ b_{ef}\ (l_p\ /\ (1 - (l_p\ /\ h)^3))^{0.5}\ k_{ar}\ k_{hm}) \tag{7}$$

$$\text{with } b_{ef} = \min \{2\ l_{ef} \tan 15^\circ;\ b\};\ k_{ar} = \min \{1 + 0.75\ (a_r\ /\ h);\ 2.0\} \tag{8}$$

$$\text{and } k_{hm} = 1 + 0.75\ l_{ef}\ /\ (1 + l_{ef}) \tag{9}$$

Acc. to prEC 5 (2021), the characteristic joint capacity, $F_{t,90,prEN,k}$, is given acc. to Eq. (10), which considers the material factor k_{mat} and the density factor k_G acc. to Eq. (11) and the effective width b_{ef}, which was interpreted by the authors in analogy to glued-in rods and acc. to Eq. (8).

$$F_{t,90,prEN,k} = k_{mat}\ k_G\ b_{ef}\ (h_e\ /\ (1 - h_e\ /\ h))^{0.5} \tag{10}$$

$$\text{with } k_{mat} = \{0.6 \text{ for ST; } 0.8 \text{ for GLT; } 1.0 \text{ for parallel LVL}\};\ k_G = (0.05\ \rho_k + 2) \tag{11}$$

Following the proposal for the block shear failure mechanism of Blaß et al. (2019), the lateral resistance of the joint volume against rolling shear stresses can be calculated acc. to Eq. (12), again with l_{ef} substituted by l_p.

$$F_{r,90,Blaß} = 2\ l_p\ (1.5\ l_p + (r - 1)\ a_1)\ b\ /\ (b - (s - 1)\ a_2)\ f_r \quad (12)$$

In general, also row shear might become a relevant failure mechanism. As this failure mechanism was neither observed in joints tested acc. to the geometric conditions in EC 5 (2014) nor ETAs, it is not considered further.

3 RESULTS AND DISCUSSION

3.1 Data sets

For the validation of the proposed block shear model, meanwhile, a valuable amount of experimentally determined data sets is available, which comprises configurations with near, in-between and distant supports, done by Plieschounig (2010), Schoenmakers (2010), Mahlknecht (2011), Mahlknecht and Brandner (2013), Mahlknecht and Brandner (2019), Ringhofer and Schickhofer (2015) and Mahlknecht et al. (2022). As already stated earlier, not all tests featured 1st failures. In such cases $R_{90,test} = F_{1st}$ applies. Data sets of Koch (2018), as presented in Blaß and Flaig (2019), are listed as well, although they don't fulfil the geometric minimum conditions acc. to EC 5 (2014) or various ETAs. Furthermore, they used beech-LVL instead of a steel plate as outer member and analysed only the maximum load from their tests. From the corresponding test curves, however, load-drops prior reaching the maximum load could be observed similar to own test experiences and the load corresponding to this first failure is evaluated. In the following, only data sets, which fulfil the required geometric conditions acc. to EC 5 (2014) or various ETAs are considered. Outcomes from testing screws of three producers featuring the same joint design and test setup (series s15_A; s15_B) are summarised to two series. Data sets featuring withdrawal or steel failure mechanism in experiments and model predictions are omitted. For these data sets a congruent and safe prediction is concluded.

3.1 Evaluation of the model

Table 3.3 lists per series the settings of the main parameters {l_{emb}; l_{ef}; d; a_1; a_2; n} and classifies the support distance and the observed failure mechanisms together with the number of observations. Furthermore, corresponding capacities $F_{1st,mean}$ and $F_{1st,min}$ or $F_{1st,05}$, last in case of > 8 # replicants per failure mechanism, are specified. Based on the stochastic-mechanical model mean and 5 %-quantile values are provided: (i) for the relevant single screw failure mechanism, min {$n\ F_{ax,sgl}$; $n\ F_{tens,sgl}$}, (ii) the resistance against block shear $F_{BS,1st}$ acc. to Section 2.2, (iii) the resistance against tension perpendicular-to-the-grain $F_{t,90,Blaß}$ acc. to Eq. (5), and (iv) the resistance against rolling shear $F_{r,90,Blaß}$ acc. to Eq. (12). For (iii) and (iv) the strength values are taken out of the stochastic modelled material properties. A view on the resulting strength values as well as the reference and block shear failure plane dimensions areas as basis for the corresponding strengths is given in Table 3.1. In Table 3.3, the **bold ratios/values** are derived from min $R_{90,pred(r,t)}$ = {$n\ F_{slg}$; $F_{t,90,Blaß}$; $F_{r,90,Blaß}$}. <u>Underlined ratios/values</u> are derived from $R_{90,pred(BS)}$ = min {$n\ F_{slg}$; $F_{BS,1st}$}.

Table 3.1 Range of area dimensions, reference areas for determination of strength values acc. to EN 408 (2012) and range in statistics (mean and 5 %-quantile values) of strength from stochastic-mechanically modelled test series; ft,90 and fv in dependence of the area of the affected plane.

area [mm²]	A_{ref} [N/mm²]	mean values [N/mm²]	5 %-quantile values [N/mm²]	timber product
$3{,}600 \le A_{t,90} \le 25{,}200$	3,150	$1.4 \le f_{t,90,mean} \le 2.0$	$0.9 \le f_{t,90,05} \le 1.3$	solid timber
$567 \le A_{t,90} \le 18{,}432$	25,000	$1.3 \le f_{t,90,mean} \le 2.6$	$0.9 \le f_{t,90,05} \le 1.7$	glulam
$4{,}800 \le A_{sr} \le 27{,}600$	-	$f_{r,mean} = 1.9$	$f_{r,05} = 1.3$	solid timber; glulam
$4{,}800 \le A_{ss} \le 14{,}400$	9,600	$6.7 \le f_{v,mean} \le 8.5$	$5.2 \le f_{v,05} \le 6.6$	solid timber
$1{,}440 \le A_{ss} \le 15{,}872$	-	$5.8 \le f_{v,mean} \le 9.4$	$4.5 \le f_{v,05} \le 7.4$	glulam

3.2.1 Mean value

In Figure 3.1 mean values from the tests including the 95 % confidence interval CI_{95} are compared with: (left) the suggested mean model predictions $R_{90,pred(BS),mean}$ and (right) the model predictions $R_{90,pred(r,t),mean}$ following the proposal of Blaß et al. (2019). If the predicted match with the mainly observed failure mechanism, the data points are additionally marked. As at tests of two series the main crack pattern and load-deformation curves indicates a mixed failure mechanism, tension perpendicular-to-the-grain and block shear (TB, series h21_E) or withdrawal and block shear (WB, series BS11), they were assigned to block shear as well. $R_{90,pred(r,t),mean}$ covers block shear either by the tension perpendicular-to-the-grain or the rolling shear failure. But, as this failure mechanisms are independently from each other and additionally observed in diverse test series, in Figure 3.1 (left) $R_{90,pred(r,t),mean}$ doesn't mark the block shear matches. For all the series, which failed mainly in block shear also block shear as failure is predicted at $R_{90,pred(BS),mean}$ together with a resistance which is estimated somewhat conservatively in total ($F_{BS,1st,mean}$ / $R_{90,test,mean}$ ≥ 0.7); average bias of all data ($R_{90,pred\ (BS),mean}$ / $R_{90,test,mean}$): mean | CoV = 0.9 | 0.16. The outcome for $R_{90,pred(BS),mean}$ clearly demonstrates that the supposed model is able to predict average resistances and failure mechanisms reliable for the majority of test series. The outcome for $R_{90,pred(r,t),mean}$ demonstrates a widely similar prediction quality of the resistance, however, predict for 36 % of the series, which failed mainly in block shear single screw failure; average bias of all data ($R_{90,pred\ (r,t),mean}$ / $R_{90,test,mean}$): mean | CoV = 1.13 | 0.19.

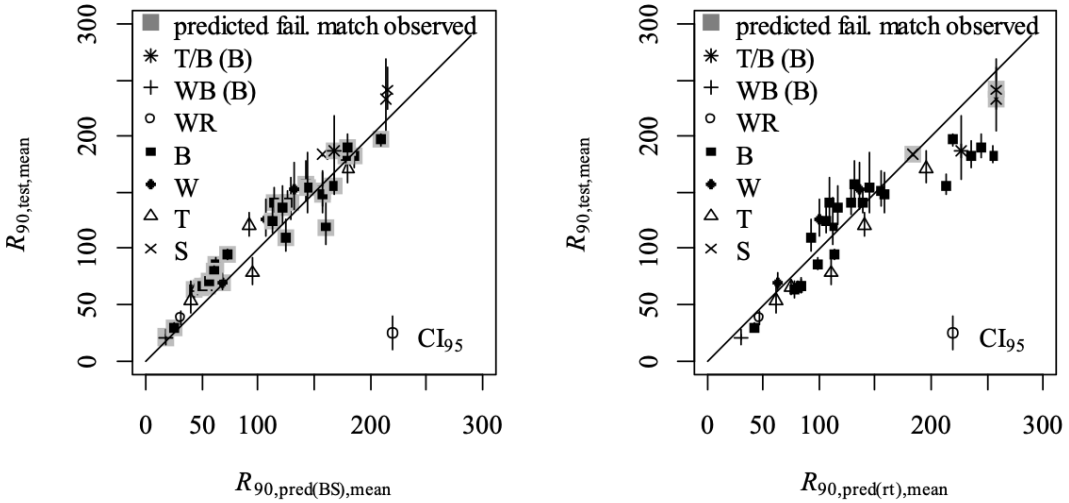

Figure 3.1 mean values R90,test,mean and corresponding confidence intervals (CI95) vs. mean values R90,pred,mean predicted from supposed models: (left) R90,pred(BS),mean; (right) R90,pred(r,t),mean.

3.2.2 Coefficients of variation from experiments and model predictions

Before analysing 5 %-quantiles, the coefficients of variation CoV of all available test series with at least eight repetitions and all apart maximum one specimen failing in block shear, with $R_{90,test} = F_{BS,1st,test}$', are compared to that of the stochastic-numerical model, CoV[$F_{BS,1st,pred}$]; see Table 3.2. All tests were done with self-tapping screws in solid timber (C24 acc. to EN 338, 2016) or glulam (GL 24h acc. to EN 14080, 2013) and fulfil the geometric conditions acc. to EC 5 (2014) or various ETAs. More details of each series are provided in Table 3.3. In the residual series, experiments featuring other failure mechanisms than block shear are treated as right-censored; corresponding statistics for these series are estimated by means of the maximum likelihood method for right censored, lognormally distributed data.

Looking at Table 3.2, the values 0.04 ≤ $CoV_{MLE}[R_{90,test}]$ ≤ 0.12 for glulam appear rather low compared to the resistance associated with other brittle timber failure mechanisms; even the coefficients of variation for the rather brittle timber strengths, e.g. CoV[f_i] ≥ 0.15 in Table 2.2, are much higher. In contrast, the values of CoV[$F_{BS,1st,pred}$] are by a factor 1.5 to 3 higher and somewhat better agree with the expectations. Those test series with unexpected low values of $CoV_{MLE}[R_{90,test}]$ show also rather low variations in the density with CoV[ρ] ≤ 5 %. This indicates a very homogeneous material, used for those test series. This circumstance is further

strengthened by positioning screw groups in almost only knot free solid timber in series s10 and s11 (to prevent force concentrations in knots), by using almost only knot free lamellas for the glulam specimens in series s15 and by producing specimens out of only a limited number of glulam beams (≤ 5) with length 12.5 m in series f13. Consequently, the applied sampling procedures led to very homogeneous but less representative test series in respect to variations in test outcomes. The comparable higher coefficients of variation in simulated series appear rather realistic but lead to more conservative results for quantiles of p < 50 %.

Table 3.2 Coefficient of variation $CoV_{MLE}[R_{90,test}]$ of test series with ≥ 8 replicates, all apart maximum one failing in block shear, compared to model predictions $CoV[F_{BS,1st,pred}]$.

series	s10 C	s10 D	s11 H	s11 I	s11 J	s12 K	s15 A	s15 B	s15 E	s15 G	s15 H	s15 I	f13 K	f13 I	f13 J
failures [a)]	9	10	9	10	9	8	30	29	10	10	10	10	10	13	15
	10	10	9	10	9	8	30	30	10	10	10	10	10	15	15
$CoV_{MLE}[R_{90,test}]$	0.18	0.27	0.19	0.17	0.14	0.10	0.08	0.10	0.04	0.09	0.07	0.09	0.08	0.07	0.09
$CoV[F_{BS,1st,pred}]$	0.16	0.16	0.25	0.25	0.26	0.15	0.25	0.26	0.13	0.20	0.20	0.26	0.20	0.20	0.20
CoV[ρ]	0.15	0.09	0.10	0.08	0.11	0.03	0.03	0.04	0.02	0.07	0.04	0.03	0.04	0.05	0.05
timber product	ST	ST	ST	ST	ST	GLT	GLT	GLT	GLT	GLT	GLT	GLT	GLT	GLT	GLT
knot free zone	✓	✓	✓	✓	✓	-	✓	✓	✓	✓	✓	✓	-	-	-
≤ 5 raw glulam beams (12.5 m)	-	-	-	-	-	-	-	-	-	-	-	-	✓	✓	✓

[a)] the upper value indicates the no. of block shear failures, the lower the total no. of tests per series

3.2.3 5 %-quantiles from experiments and model predictions

Analogue to the mean values in Figure 3.1, Figure 3.2 compares the 5 %-quantile values from test series, $R_{90,test,05}$, based on a lognormal distribution, vs. the 5 %-quantile values from the model predictions $R_{90,pred,05}$ (with $F_{BS,1st,05}$*). As for the mean values, the outcomes of the supposed model, $R_{90,pred(BS),05}$ in Figure 3.2 left, predict pretty well the per series dominating failure mechanisms and the corresponding resistances are overall somewhat conservative in trend, which, as discussed in Section 3.2.2, was expected. For all of the series, which failed mainly in block shear also block shear is predicted at $R_{90,pred(BS),05}$. $R_{90,pred(r,t),05}$ in Figure 3.2 right appears partly less conservative and for 64 % matches brittle timber failure for observed mainly block shear mechanism. The number of withdrawal failure predictions, although the main observed mechanism was block shear, will increase by following the rules in EC 5 (2014) and various ETAs, because in the made comparison $n_{ef} = n$.

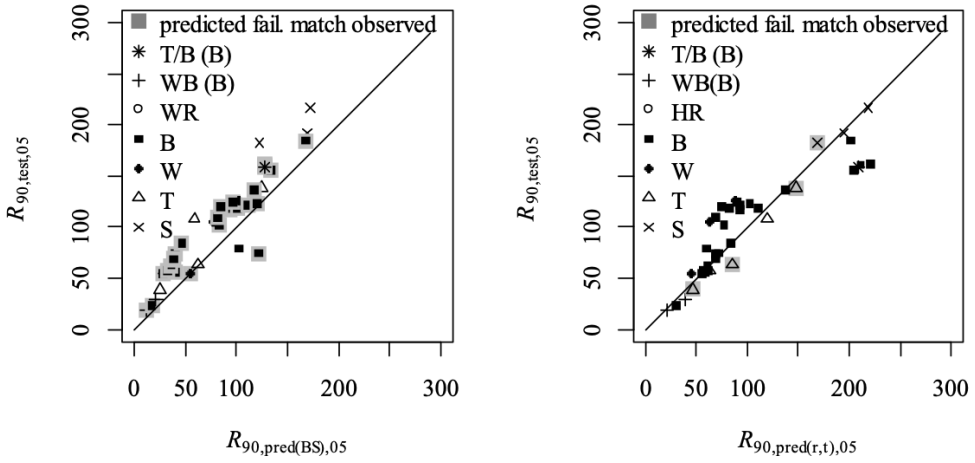

Figure 3.2 5 %-quantil values $R_{90,test,05}$ vs. 5 %-quantil values $R_{90,pred,05}$, both based on lognormal distribution, predicted from supposed models: (left) $R_{90,pred(BS),05}$ and (right) $R_{90,pred(r,t),05}$

Table 3.3. Statistics of test results and model predictions from series dominated by / solely featuring block shear failures

series	$(l_{emb}+l_{ef} \mid a_1 \mid a_2)$ / d; n	failure$_{no.\ of\ replicants}$	$R_{90,test,05}$ [kN]	$R_{90,test,mean}$ [kN]	$n\,F_{sgl,mean}$ [b] / $R_{90,test,mean}$	$F_{r,90,Blaß,mean}$ / $R_{90,test,mean}$	$F_{t,90,Blaß,mean}$ / $R_{90,test,mean}$	$F_{BS,1st,mean}$ / $R_{90,test,mean}$	$n\,F_{sgl,05}$ [b] [kN]	0.9 n $F_{sgl,05}$ [b] [kN]	$n_{ef,EC5}$ $F_{sgl,05}$ [b] [kN]	$F_{r,90,05}$ [kN]	$F_{t,90,Blaß,05}$ [kN]	$F_{BS,1st,05}$ [kN]
$_{s10_}$B	2+11.3 | 5 | 5; 9	W_6 B_4	64 54	70	0.98	0.91	1.12	1.27	55	50	44	45	52	67
$_{s10_}$C	2+11.3 | 5 | 5; 16	W_1 B_9	133 104 [a]	110	1.16	0.93	0.85	1.13	102	92	77	72	60	95
$_{s10_}$D	2+11.3 | 5 | 5; 25	B_{10}	110 [a]	119	1.74	1.54	0.95	1.35	153	136	109	131	72	122
$_{s11_}$C	25.7 | 5 | 5; 16 h = 252 mm	S_3 B_2	239 191	234	1.10	1.32	1.30	0.92	199	176	149	217	195	169
$_{s11_}$D	25.7 | 5 | 5; 16 h = 163 mm	S_4 B_1	246 215	242	1.07	1.28	38.1	0.89	206	182	154	218	5916	172
$_{s11_}$H	4+11.3 | 7.5 | 3.5; 25	B_9	134 [a]	141	1.30	0.77	0.97	0.91	146	131	106	77	87	83
$_{s11_}$I	4+11.3 | 10 | 3.5; 25	B_{10}	151 [a]	157	1.18	0.84	0.99	0.91	148	133	107	93	100	93
$_{s11_}$J	4+11.3 | 12.5 | 3.5; 25	B_9	146 [a]	151	1.21	1.02	1.15	1.04	146	131	106	110	112	101
glulam GL 24h acc. to EN 14080 (2013); data of Koch (2018)/Blaß and Flaig (2019); geometric conditions acc. to EC 5 (2014) or var. ETAs not fulfilled; near support														
BS11	9 | 4 | 4; 4; d = 6 mm	WB_5 WR_1	18.6 21.8	21	1.47	1.42	4.42	0.82	26	22	23	21	59	12
BS12	9 | 4 | 4; 8; d = 6 mm	B_5 WB_1	25.6 24.0	29	2.06	1.44	4.24	0.87	50	45	41	30	80	17
BS21	9 | 4 | 4; 4; d = 8 mm	WR_6	31.5	38	1.23	1.47	8.44	0.83	39	35	34	39	205	21
BS22	9 | 4 | 4; 8; d = 8 mm	B_5	55.2	63	1.56	1.23	7.16	0.67	82	74	67	56	293	28
BS31	14 | 4 | 4; 8; d = 6 mm	B_5	60.9	65	1.34	1.24	12.1	0.76	73	65	59	57	528	37
BS32	14 | 4 | 5; 8; d = 6 mm	B_6	58.2	66	1.35	1.26	12.4	0.82	75	67	61	59	534	40
glulam GL 28h acc. to EN 14080 (2013); data of Schoenmakers (2010) ; distant support														
Sc_c	8 | 8 | 8; 6; d = 8 mm	T_5	45.4	54	1.13	2.81	1.35	0.74	51	46	43	105	47	25
Sc_d	14 | 8 | 8; 6; d = 8 mm	T_5	69.3	78	1.42	4.49	1.70	1.22	94	85	79	246	86	63
Sc_g	5 | 8 | 8; 6; d = 12 mm	T_5	56.6	65	1.53	1.91	1.58	0.70	63	56	52	88	66	29
Sc_h	9 | 8 | 8; 6; d = 12 mm	T_5	107.5	121	1.53	2.29	1.53	0.76	119	108	100	197	120	59
glulam GL 24h acc. to EN 14080 (2013); near support														
$_{s12_}$C	28.3 | 10 | 2.5; 12; d = 6 mm	S_4 B_1	184 182	184	1.00	1.90	2.10	0.86	169	152	132	248	251	123
$_{s12_}$K	17.8 | 7.5 | 3.5; 12; d = 6 mm	B_8	123 [a]	141	1.10 [d]	1.23	0.91	0.81	115 [d]	139	120	124	83	88

series	$(l_{emb}+l_{ef} \mid a_1 \mid a_2)$ / d; n	failure$_{no.\ of\ replicants}$	$R_{90,test,05}$ [kN]	$R_{90,test,mean}$ [kN]	$n\,F_{sgl,mean}$ [b] / $R_{90,test,mean}$	$F_{r,90,Blaß,mean}$ / $R_{90,test,mean}$	$F_{t,90,Blaß,mean}$ / $R_{90,test,mean}$	$F_{BS,1st,mean}$ / $R_{90,test,mean}$	$n\,F_{sgl,05}$ [b] [kN]	0.9 $n\,F_{sgl,05}$ [b] [kN]	$n_{ef,EC5}$ $F_{sgl,05}$ [b] [kN]	$F_{i,90,05}$ [kN]	$F_{t,90,Blaß,05}$ [kN]	$F_{BS,1st,05}$ [kN]
s12_L	17.8 | 10 | 3.5; 12; d = 6 mm	B_7 W_1	130 164	141	1.09 [d]	1.38	0.99	0.90	115 [d]	138	120	136	90	97
s12_M	17.8 | 5 | 5; 12; d = 6 mm	B_1 W_4	124 154	153	1.01 [d]	1.30	0.88	0.86	115 [d]	138	119	140	88	102
s12_N	17.8 | 7.5 | 5; 12; d = 6 mm	B_2 W_2 [c]	126 156	155	1.04 [d]	1.45	0.94	0.93	119 [d]	143	12w4	160	93	111
s12_O	17.8 | 10 | 5; 12; d = 6 mm	B_3 W_2 [c]	130 148	148	1.06 [d]	1.71	1.06	1.06	117 [d]	140	122	178	102	120
s12_S	14.2 | 5 | 5; 12; d = 6 mm	B_2 W_3	112 129	126	1.00 [d]	1.10	0.80	0.84	92 [d]	107	93	98	63	77
s12_T	14.2 | 7.5 | 5; 12; d = 6 mm	B_5	109	124	1.00 [d]	1.26	0.85	0.91	92 [d]	106	92	111	69	81
s12_U	14.2 | 10 | 5; 12; d = 6 mm	B_2 W_2	123 134	137	1.05 [d]	1.33	0.85	0.89	96 [d]	111	96	129	75	84
s15_A	8.8 | 5 | 5; 9; d = 8 mm	B_{30}	69 [a]	71	1.24	1.23	1.60	0.80	73	66	59	61	73	36
s15_G	8.8 | 5 | 5; 12; d = 8 mm	B_{10}	84 [a]	86	1.35	1.16	1.53	0.73	97	87	76	68	85	40
s15_B	8.8 | 7 | 5; 9; d = 8 mm	B_{29} W_1	79 [a] 97	80	1.07	1.21	1.52	0.73	73	66	58	69	80	39
s15_H	8.8 | 7 | 5; 12; d = 8 mm	B_{10}	93 [a]	94	1.20	1.26	1.61	0.77	95	86	74	84	98	46
s15_I	8.8 | 10 | 2.5; 9; d = 8 mm	B_{10}	65 [a]	67	1.25	1.32	1.89	0.75	70	63	56	62	81	32
s15_E	24.8 | 7 | 5; 9; d = 8 mm	B_{10}	195 [a]	197	1.11	2.50	2.08	1.07	202	182	162	348	267	168
glulam GL 24h acc. to EN 14080 (2013); screws with d = 8 mm; distant support														
f13_N	18.5 | 10.5 | 5; 8	B_3 T_5 R_2	127 165 167	171	1.14	2.29	1.32	1.05	168	151	137	273	147	124
f13_K	18.5 | 5.3 | 5; 10	B_{10}	153 [a]	156	1.47	2.31	1.36	1.07	198	178	157	256	137	117
f13_O	18.5 | 5.3 | 5; 10	B_6 T_1 R_3	162 169 155	183	1.29	1.98	4.23	1.02	204	184	162	255	502	133
f13_I	18.5 | 7.9 | 3.3; 10	B_{13} R_2	182 [a] 172	183	1.40	1.86	4.09	0.97	221	199	175	241	497	128
f13_J	18.5 | 5.3 | 5; 10	B_{15}	186 [a]	190	1.29	1.82	3.97	0.95	211	190	168	246	483	128
h21_E	31.5 | 10 | 2.5; 6	TB_4	164	187	1.21	2.98	2.01	0.90	209	188	175	398	243	128

W … withdrawal; B … block shear; T … tension perpendicular-to-the-grain; S … screw tension; R … rolling shear; mixed failure: TB … block shear / tension perpendicular-to-the-grain, WB … withdrawal / block shear, WR … withdrawal / rolling shear; [a] for ≤ 8 # replicants $F_{1st,min}$; [b] $F_{tens,sgl}$ only if relevant, otherwise $F_{ax,sgl}$; [c] one test failed by screw tension

d) due to a later data correction values of INTER 2022 publication deviate, but without any impact on presented results, see even Mahlknecht (pr2023)

4 SIMPLIFIED BLOCK SHEAR MODEL

The proposed block shear model in its comprehensive version might be probably too cumbersome for the daily practice. Furthermore, material parameters as implemented in this model are usually not available for the designers, which have to rely on characteristic properties tabulated in product and design standards. With focus on ease-of-use, the aim is to elaborate a simplified version. Therefore, some additional boundary conditions and limits are set:

- In view of typical practical applications, only distant support conditions are considered. Resulting from this: $C_{t,90} = 0.5$; $C_t = C_s = C_r = 1.0$; $X_r = 2.5\ d$; $X_s = (10 - 5\ l_p / h)\ d$
- So far, rolling shear properties are only provided for glulam in EN 14080 (2013), with $G_{r,mean} = 65$ N/mm² and $f_{r,k} = 1.2$ N/mm². These values are clearly different to $G_{r,mean} = 100$ N/mm² and $f_{r,k} = 1.3$ N/mm² used so far in the model. To adjust the currently regulated properties to currently proposed values, the factors $k_{r,G} = 1.5$ and $k_{r,f} = 1.1$ apply in the simplified model; see Eq. (16) and (17).
- For all softwood solid timber strength classes acc. to EN 338 (2016) $f_{t,90,k} = 0.4$ N/mm², and for classes higher than C22 $f_{v,k} = 4.0$ N/mm² apply. EN 14080 (2013) gives constant strength values $f_{t,90,k} = 0.5$ N/mm² and $f_{v,k} = 3.5$ N/mm² for all glulam strength classes. These values are again clearly below the more realistic material properties used so far in the model (see Table 3.1). Current regulations also not account for size effects, i.e. the dimension of $A_{t,90}$ and $A_{s,s}$. As $f_{t,90}$ turned out to be the dominating property for the block shear resistance adequate basic values and their adjustment to $A_{t,90}$ are mandatory. In respect to the latter, the size effect can be regulated analogue to the volume factor k_{vol} of EC 5 (2014) or similar to the model of $F_{t,90,Blaß}$ via $(A_{t,90,ref} / A_{t,90})^{0.2}$. As the depth of the failure plane is clearly defined in case of block shear, i.e. at the screw tips, for solid timber and glulam the same properties apply which are set acc. to Ehlbeck et al.(1989). To adjust them accordingly to characteristic properties currently regulated in EN 338 (2016) and EN 14080 (2013) following applies: $k_{t,90} = 2.4\ (3{,}150 / A_{t,90})^{0.2}$ for solid timber and $k_{t,90} = 3.0\ (3{,}150 / A_{t,90})^{0.2}$ for glulam. An analogue size effect applies also for the shear strength with $k_v = 1 / f_{v,k}$ min $\{4.0\ (150 / h_b)^{0.2}; 4.5\}$ for solid timber and $k_v = 1 / f_{v,k}$ min $\{3.5\ (600 / h_b)^{0.2}; 4.0\}$ for glulam acc. to Brandner et al. (2012); see Eq. (17).

Consequently, Eqs. (13) to (17) summarise the simplified block shear model.

$$A_{t,90} = (r - 1)\ a_1\ (s - 1)\ a_2;\ A_{s,s} = (s - 1)\ a_2\ h_b;\ A_{s,r} = (r - 1)\ a_1\ h_b \tag{13}$$

with $h_b = 0.5\ l_{emb} + l_{ef}$

$$K_{t,90} = 2\ E_{t,90,mean}\ A_{t,90} / h_b \tag{14}$$

$$K_s = G_{0,mean}\ A_{s,s} / X_s + E_{t,90,mean}\ A_{t,s} / (10\ h_b) \tag{15}$$

with $A_{t,s} = (s - 1)\ a_2\ X_s$ and $X_s = (10 - 5\ l_p / h)\ d$

$$K_r = 0.4\ k_{r,G}\ G_{r,mean}\ A_{s,r} / d + E_{t,90,mean}\ A_{t,r} / (10\ h_b),\ \text{with } A_{t,r} = 2.5\ d\ (r - 1)\ a_1 \tag{16}$$

$$F_{BS,05} = (K_{t,90} + 2\ K_s + 2\ K_r)\ \min\{k_{t,90}\ f_{t,90,k}\ A_{t,90} / K_{t,90};\ k_v\ f_{v,k}\ A_{s,s} / K_s;\ k_{r,f}\ f_{r,k}\ A_{s,r} / K_r\} \tag{17}$$

Figure 4.1 compares the block shear test data of series done in glulam with close (s15), in-between (f13, BS) and distant (h21) support, with single resistance $F_{sgl,05}$ considering n, n_{ef} acc. to EC 5 (2014), the 5% quantile of test loads determined acc. to EN 14358 (2016) $F_{test,05EN14358}$, the simplified block shear resistance $F_{BS,05}$, min ($F_{r,90,Blaß,05}$; $F_{t,90,Blaß,05}$) and with both resistances regulated for beams/hangers against tension perpendicular-to-the-grain, $F_{t,90,prEN,k}$ and $F_{t,90,SIA,k}$, by means of f_i acc. to EN 14080 (2013); all values referenced to n $F_{sgl,05}$.

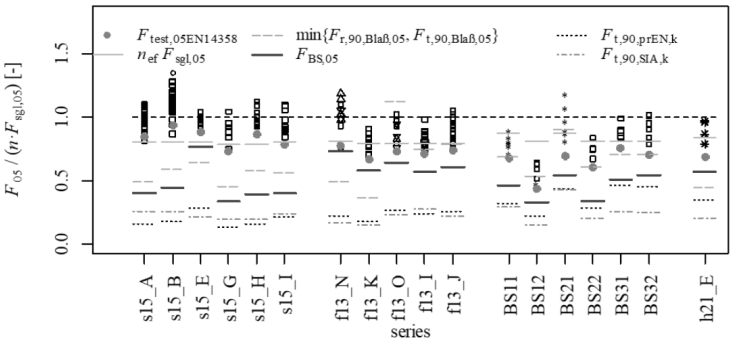

Figure 4.1 comparison of test data from series in glulam with close (s15), in-between (f13, BS) and distant support (h21), which failed solely or primary in block shear with various model predictions on characteristic (5 %-quantile) level.

The comparison outlines the necessity to consider brittle timber failure modes, even for joints which fulfil the conditions acc. to EC 5 (2014) and various ETAs (s15_, f13_ and h21_E). Regarding the block shear model predictions of Blaß et al. (2019), with $R_{90,05}$ = min {n_{ef} $F_{sgl,05}$, $F_{r,90,Blaß,05}$; $F_{t,90,Blaß,05}$}, the results are shortly progressive; however, considering realistically a higher scatter they become even more. This is especially apparent for series featuring l_p > 0.7 h (e.g. series f13_O, f13_I and f13_J). The simplified block shear model, with $R_{90,05}$ = min {n_{ef} $F_{sgl,05}$, $F_{BS,05}$}, gives results on the safe side, which, considering the area of application of this model, are consistent for series featuring in-between and distant support conditions. The model is somewhat conservative for the near supporting (s15) and for series with l_p < 0.7. The models acc. to prEC (2021) and SIA (2021) give overall very conservative results.

5 CONCLUSIONS

Generally, the aim to end up in joint failure mechanisms whose properties are well-known from single screws and easy to determine has clearly the benefit of ease-of-use. For axially-loaded screw groups in softwood Mahlknecht and Brandner (2019) noted: (i) for l_{ef} up to 20 d withdrawal is usually the leading failure mechanism as long as the spacing complies with EC 5 (2014) and the number of screws in a row in grain is $r \leq 3$, and (ii) for screw groups prone to fail in steel, the current regulation a_1 $a_2 \geq 25$ d^2 can be applied as long as $a_1 \geq 5$ d and $a_2 \geq 3.5$ d and F_{model} > (1.05 n F_{tens}) are fulfilled. Mahlknecht et al. (2021) confirm these principle findings also for applications in hardwoods. If the recommendations cannot be followed, there might be a risk for brittle timber failure mechanisms. This was demonstrated for various group parameter settings which lead to failure in block shear or tension perpendicular-to-the-grain, even at penetration lengths l_p > 0.7 h. The rule to be safe from brittle timber failure mechanisms in joints featuring l_p > 0.7 h in the national annexes of Austria (ÖNORM B 1995-1-1, 2019) and Germany (DIN EN 1995-1-1/NA, 2013) is seen critically. Anyhow, this recommended penetration length should be applied also in joints with axially-loaded screws.

The advantage of the proposed block shear model is its flexibility in respect to material properties and group dimensions. Even joints with >> $a_{2,CG}$, as e.g. wind bracing joints situated on member's side-face can be represented accordingly. Additionally, the proposed block shear model predicts the experimentally observed failure mechanism with high accuracy. The simplified model on the characteristic (5 %-quantile) level adapts standardized characteristic properties to realistic ones (evident by a large amount of experimental test results) in an explicit, comprehensible manner and thus enables an objective adjustment of any pre-factors and formulations in the event of changes in these. The model gives safe predictions for all available series, especially for series with l_p > 0.7 h. The models acc. to prEC (2021) and SIA (2021) for the resistance of joints in beams/hangers loaded perpendicular-to-the-grain give overall very conservative predictions.

6 ACKNOWLEDGEMENTS

The current investigations are part of the European Research Area Networking (ERA-NET) project FOREST VALUE hardwood_joint project with funding by European Union. Thank goes to the scientific project partners of Karlsruhe Institute of Technology (KIT; leader) in Germany, Linneaus University in Sweden, Universite de Lorraine in France and commercial partners Schmid Schrauben Hainfeld GmbH, Adolf Würth GmbH & Co. KG, Pollmeier Furnierwerkstoffe GmbH and Hasslacher Group for their valuable input. Preceded work took place in the extent of the FFG projects BRIDGE-SCREWS (2010–2012; No. 824929) at Graz University of Technology and COMET-K

“focus_sts” (2013–2016; No. 836619) at holz.bau forschungs gmbh in Graz.

7 REFERENCES

Blaß HJ, Ehlbeck J, Schmid M (1998) Ermittlung der Querzugfestigkeit von Voll- und Brettschichtholz. Technical Report, Universität Karlsruhe, Germany (in German).

Blaß HJ, Flaig M (2019) Blockscheren von Holzbauteilen im Verbindungsbereich axial beanspruchter Vollgewindeschrauben. Karlsruher Berichte zum Ingenieurholzbau, Band 35, KIT, Germany (in German).

Blaß HJ, Flaig M, Meyer N (2019) Row shear and block shear failure of connection with axially loaded screws. INTER/52-07-6, Tacoma, USA.

Brandner R (2012) Stochastic system actions and effects in engineered timber products and structures. Dissertation, TU Graz, Austria.

Brandner R, Gatternig W, Schickhofer G (2012) Determination of shear strength of structural and glued laminated timber. CIB-W18/45-12-2, Växjö, Sweden.

Carradine DM, Newcombe MP, Buchanan AH (2009) Using screws for structural applications in laminated veneer lumber. CIB-W18A/42-7-7, Duebendorf, Switzerland.

Dietsch P, Brandner R (2015) Self-tapping screws and threaded rods as reinforcement for structural timber elements – A state-of-the-art report. Constr Build Mater 97, pp. 78-89.

DIN EN 1995-1-1/NA:2013 Nationaler Anhang – National festgelegte Parameter – Eurocode 5: Bemessung und Konstruktion von Holzbauten – Teil 1-1: Allgemeines – Allgemeine Regeln und Regeln für den Hochbau. DIN.

EC 5 (2014) – EN 1995-1-1:2004 + AC:2006 + A1:2008 + A2:2014 Eurocode 5: Design of timber structures – Part 1-1: General – Common rules and rules for buildings. CEN.

Ehlbeck J, Görlacher R, Werne H (1989) Determination of perpendicular-to-grain tensile stresses in joints with dowel-type fasteners. CIB-W18A/22-7-2, Berlin, Germany.

Ehrhart T, Brandner R (2018) Rolling shear: test configurations and properties of some European soft- and hardwood species. Eng Struct 172, pp. 554-572

EN 338 (2016) Structural timber – Strength classes. CEN.

EN 408 (2010+A1) Timber structures – Structural timber and glued laminated timber – Determination of some physical and mechanical properties. CEN

EN 14080 (2013) Timber structures – Glued laminated timber and glued solid timber - Requirements. CEN.

EN 14358 (2016) Timber structures – Calculation and verification of characteristic values. CEN.

JCSS (2006) JCSS probabilistic model code – Part 3: resistance models – 3.5 properties of timber. Joint Committee on Structural Safety.

Koch E (2018) Blockscheren von Holzbauteilen. Master Thesis, KIT, Germany (in German).

Krenn H (2017) Die Stahlblech-Holz-Laschenverbindung mit schrägen Schrauben. Dissertation, TU Graz, Austria (in German).

Leijten AJM, Jorissen A (2001) Splitting strength of beams loaded by connections perpendicular to grain, model validation. CIB-W18/34-7-1, Venice (I)

Mahlknecht U (prospective 2023) Blockscheren am Queranschluss einer axial beanspruchten Schraubengruppe. Dissertation, TU Graz, Austria (in German).

Mahlknecht U, Brandner R (2013) focus_sts 3.1.2 Untersuchungen des mechanischen Verhaltens von Schrauben – Verbindungsmittelgruppen in VH, BSH und BSP – Forschungsbericht. HBF gmbh and TU Graz, Austria (in German).

Mahlknecht U, Brandner R (2019) Block shear failure mechanism of axially-loaded groups of screws. Eng Struct 183(2019) 220-242.

Mahlknecht U, Brandner R, Augustin M (2016) Block shear failure mode of axially loaded groups of screws. WCTE 2016, Vienna, Austria.

Mahlknecht U, Brandner R, Ringhofer A (2021) Minimum geometric and execution conditions for axially loaded groups of screws in hardwood. INTER/54-07-7, online.

Mahlknecht U, Brandner R, Ringhofer A (2022) Queranschluss mit axial beanspruchten Schraubengruppen am Einfeldträger aus Laubholz und Fichte. Technical Report, TU Graz, Austria (in German).

Mahlknecht U, Brandner R, Ringhofer A, Schickhofer G (2014) Resistance and failure modes of axially loaded groups of screws. RILEM Bookseries, Springer, 1 ed., Vol. 9.

Mayer N, Blaß HJ (2018) Connections with glued-in rods in trusses made of beech-LVL. WCTE 2018, Seoul, Republic of Korea.

ÖNORM B 1995-1-1:2019 Eurocode 5: Design of timber structures – Part 1-1: General – Common rules and rules for buildings – Consolidated version. ASI.

Plieschounig S (2010) Ausziehverhalten axial beanspruchter Schraubengruppen. Master Thesis, TU Graz, Austria (in German).

prEC 5 (2021) prEN 1995-1-1:2021 Comment: Consolidated draft prEN 1995-1-1, informal enquiry, Eurocode 5: Design of timber structures – Common rules and rules for buildings – Part 1-1: General. CEN.

Ringhofer A, Schickhofer G (2015) Ausziehprüfungen von Schraubengruppen in Anlehnung an das EAD 130015-00-0603, Abschnitt 2.2.1210 zur Bestimmung der Mindestabstände a_1 und a_2, Test Report Nr. PB15-471-1-01. Lignum Test Center (LTC), TU Graz, Austria (in German).

Ringhofer A, Brandner R, Schickhofer G (2015) A universal approach for withdrawal properties of self-tapping screws in solid timber and laminated timber products. INTER/48-7-1, Sibenik, Croatia.

Schoenmakers JCM (2010) Fracture and failure mechanisms in timber loaded perpendicular to the grain by mechanical connections. Dissertation, Eindhoven University of Technology, Netherlands.
SIA 265:2021 Timber Structures, Schweizerischer Ingenieur- und Architektenverein.

Zarnani P, Quenneville P (2012) Predictive analytical model for wood capacity of rivet connections in glulam an LVL. WCTE 2012, Auckland, New Zealand.